

---

---

SOIL PHYSICS

---

---

## Rheological Properties of Typical Chernozems (Kursk Oblast) under Different Land Use

D. D. Khaidapova, V. V. Chestnova, E. V. Shein, and E. Yu. Milanovskii

*Moscow State University, Moscow, 119991 Russia*

*e-mail: dkhaydapova@yandex.ru*

Received June 24, 2015

**Abstract**—Rheological parameters of humus horizons from typical chernozems under different land use—on a virgin land (unmown steppe) and under an oak forest, long-term black fallow, and agricultural use—have been studied by the amplitude sweep method with an MCR-302 modular rheometer at water contents corresponding to swelling limit and liquid limit. From the curves of elastic and viscous moduli, the ranges of elastic and viscoelastic (plastic) behavior of soil pastes—as well as that of transition from viscoelastic to viscous behavior—have been determined. It has been shown that the rheological behavior is largely determined by the content of organic matter, which can act as a binding agent structuring the interparticle bonds and as a lubricant in the viscous-flow (plastic) state of soil pastes. Soil samples enriched with organic matter (virgin land, oak forest, forest belt) have a more plastic behavior and a higher resistance to loads. Soil samples with the lower content of organic matter (long-term fallow, plowland) are characterized by a more rigid cohesion of particles and a narrower range of load resistance. Soil pastes at the water content of liquid limit have a stronger interparticle cohesion and a more brittle behavior than at the water content of swelling limit. Methodological aspects of testing soil pastes at the constant sample thickness and the controlled normal load have been considered. For swelling soil samples, tests under controlled normal load are preferred.

**Keywords:** soil rheology, amplitude sweep mode, modular rheometer, chernozem organic matter

**DOI:** 10.1134/S1064229316080044

### INTRODUCTION

The prevalent concept of soil science considers the soil structure as a combination of soil aggregates formed from elementary soil particles mutually retained due to the coagulation of colloids; their cohesion by Van der Waals forces, residual valences, and hydrogen bonds; adsorption and capillary phenomena in the liquid phase; and root cords and fungal hyphae. Two approaches referred to as morphometric and energetic are developed for the identification of structural forms in soil science [8]. In the former approach, which is most widespread, the concept of structure is based on the morphometric features of aggregates and their ratios in the soil: sizes, shapes, and mutual arrangement [6]. In the latter approach, the concept of structure is based on such parameters as the interaction of structural units; the assessment of mutual coupling and cohesion of particles; and the structure of the pore space, which is manifested in the physico-mechanical properties of soil: density, hardness, water resistance, stickiness, plasticity, shear strength, cohesion, water and air permeability, etc. In this approach, the generalizing properties of soil structure related to all soil elements (composition, size, shape, and surface of aggregate-composing soil particles, etc.) include mechanical strength and some rheological

properties of soils as viscosity, elasticity, their common manifestation, viscoelastic behavior, etc. [6, 8].

Rheological properties of soils are functional manifestations of the surface properties of the soil solid phase determining the formation, stability, and degradation of soil structure. Gor'kova, Abrukova, Manucharov and other scientists [1, 2, 7, 9] began to apply the rheological approaches to the studies of soil structure in the 1970s–1980s. Studies of the rheological properties of soils on a Rheotest-2 instrument by the coaxial cylinder method showed some interesting semiquantitative behavior parameters of soil samples, which are more closely related to viscous behavior. From the shapes of hysteresis loops formed at the increased or decreased shear rate and during recoil, the restoration of disrupted bonds and the type of structural bonds can be described [15, 21].

Instruments of a new generation have appeared recently that allow significant expansion of the number and accuracy of physically substantiated rheological parameters suitable for the determination of interaction between particles and the prediction of the behavior of soil macrostructure subjected to loads. In particular, tests in oscillation mode performed on an MCR-302 parallel-plate rheometer are suitable and recommended by some authors for the study of the

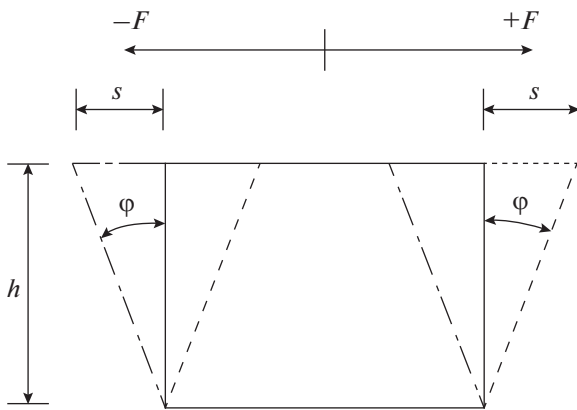


**Fig. 1.** Oscillation method: shear force  $\pm F$ , deviation distance  $\pm s$ , and deviation angle  $\pm \phi$  in the clearance between the plates  $h$  ([25]).

rheological properties of soils [13, 19, 22–24], especially in the viscoelastic region before the transition to the viscous flow region.

In this work, viscoelastic properties of typical chernozems under different land use were studied. The amplitude sweep method in oscillatory mode with a measuring system of parallel plates was used; measurements were performed on an MCR-302 modular rheometer (Anton-Paar, Austria) [25].

**Theory of the method.** The amplitude sweep method involves deformation of the sample or the application of oscillating stress. The tests with oscillating stress are frequently referred to as dynamic tests [20, 25]. They provide information on the viscous and elastic response of the sample depending on the rate of impact, or the oscillating stress or deformation depending on the set angular speed or frequency [20].

The principle of the method is that the sample is placed between two plates, and the upper plate undergoes oscillations with increasing amplitude at a constant frequency [25]. The distance  $h$  between the plates is the shear area (Fig. 1).

When the wheel turns, the upper plate shifts forth and back with the shear force  $\pm F$ . The movement of the upper plate causes the shift of the sample placed between the plates, with the indication of deviation path  $\pm s$  and deviation angle  $\pm \phi$ .

The shear stress  $\tau$  is equal to the applied force  $F$  divided by the plate area  $A$ :  $\pm \tau [\text{Pa}] = \pm F/A$ , and the shear deformation is  $\pm \gamma = \pm s/h = \pm \text{tg } \phi$ , where  $s$  is the deviation, and  $h$  is the distance between the plates.

The theoretical aspects of the methods are expanded in *The Rheology Handbook* by Mezger [25]. As shown in Fig. 2, the movement of the upper plate is caused by the rotation of the wheel motor. The resulting force is measured on the lower plate. At the complete revolution, the rotational angle is  $360^\circ$ . This corresponds to the complete oscillation cycle of time-

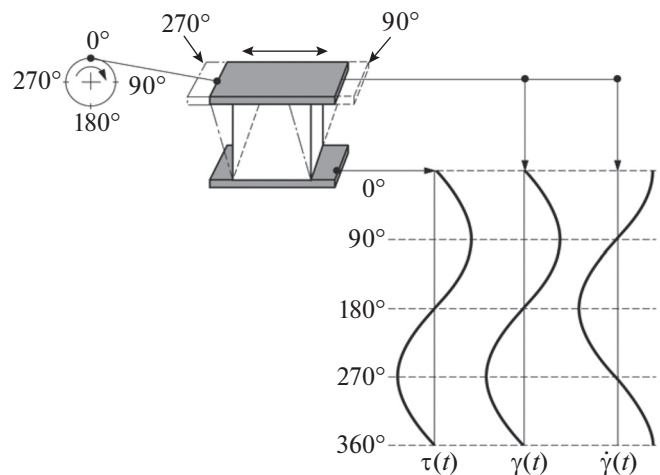


**Fig. 2.** Two-plate model in the oscillation method; ideal elastic behavior: sinusoidal and cosinusoidal time functions  $\tau(t)$ ,  $\gamma(t)$ , and  $\dot{\gamma}(t)$  ([25]).

dependent functions  $\tau(t)$  and  $\gamma(t)$  or  $\dot{\gamma}(t)$ , respectively. During the continuous rotation, when the wheel passes the angular positions of  $0^\circ$  or  $180^\circ$ , the upper plate shows the zero position; therefore,  $\gamma(t) = 0$  and  $\tau(t) = 0$ . However, the rate is maximum in this moment; i.e.,  $\dot{\gamma}(t) = \dot{\gamma}_{\max}$ . At the angular position of  $90^\circ$ , the upper plate shows the maximum deviation to the right; the maximum deviation to the left corresponds to  $270^\circ$ . Then,  $\gamma(t) = \gamma_{\max}$  and  $\tau(t) = \tau_{\max}$  or  $\gamma(t) = -\gamma_{\max}$  and  $\tau(t) = -\tau_{\max}$ , respectively. The rate is zero; i.e.,  $\dot{\gamma}(t) = 0$ , and the movement changes completely in this point. At  $G^* = \tau(t)/\gamma(t) = \text{const}$ , the  $\tau(t)$  curve is always in phase with the  $\gamma(t)$  curve; i.e., these are synchronous sinusoidal curves. Formally, the deformation can be represented as

$$\gamma(t) = \gamma_A \sin \omega t,$$

where  $\gamma_A$  is the deformation amplitude, %, and  $\omega$  is the angular frequency, rad/s or  $\text{s}^{-1}$ . The amplitude is measured from the basic zero line to the peak only on one side of the sinusoidal curve. The oscillation frequency can be represented in two ways, as angular frequency  $\omega$  (rad/s or  $\text{s}^{-1}$ ) or as frequency  $f$  (Hz). These two frequencies are related by the equation  $\omega = 2\pi f$ ; e.g.,  $f = 10$  Hz corresponds to  $\omega = 62.8$  rad/s or  $62.8 \text{ s}^{-1}$ .

For the samples showing an ideal elastic behavior, there is no delay between the  $\gamma(t)$  and  $\tau(t)$  curves, i.e., the phase shift  $\delta = 0^\circ$ .

In the case of the ideal viscous behavior, the  $\gamma(t)$  curve has a sinusoidal shape, and the  $\tau(t)$  and  $\dot{\gamma}(t)$  curves are cosinusoidal. For the samples showing an ideal viscous behavior, there is a lag between the  $\tau(t)$  and  $\gamma(t)$  curves with the phase shift of  $90^\circ$ .

In most cases, the behavior is viscoelastic. At the set deformation  $\gamma$ , the  $\tau$  curve has a sinusoidal shape  $\tau(t) = \tau_A \sin(\omega t + \delta)$  with the phase shift  $\delta$  between the

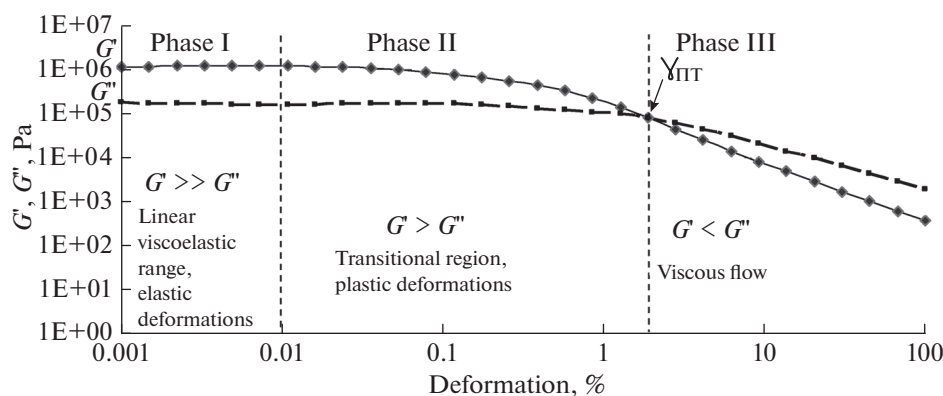


Fig. 3. Elastic modulus  $G'$  and viscous modulus  $G''$  of virgin chernozem at the liquid limit water content.

set and resulting curves. The angle  $\delta$  is usually measured in degrees. The phase shift is always between  $0^\circ$  and  $90^\circ$ :  $0^\circ \leq \delta \leq 90^\circ$ .

For the ideal elastic behavior,  $\delta = 0^\circ$ ; for the ideal viscous behavior,  $\delta = 90^\circ$ ; for the viscoelastic behavior,  $0^\circ < \delta < 90^\circ$ . At the study of viscoelastic materials, the resulting sinusoid will always show a delay from the set curve [25].

We shall briefly characterize the obtained rheological parameters: elastic modulus, viscous modulus, linear viscoelastic range, liquid limit as the intersection point of the moduli, damping factor, and integrated zone  $Z$ . The rheometer software shows the values of elastic and viscous moduli ( $G'$  and  $G''$ , respectively) in the form of tables and plots (Fig. 3).

**Elastic modulus (storage modulus)  $G'$  [Pa]** is a measure of deformation energy conserved by the sample during the shear process. After the removal of shearing stress, this energy is completely conserved and acts as a driving force for the partial or complete restoration of the previous structural deformation. The materials completely conserving the deformation energy show a behavior of complete reversible deformation after the removal of the load and have a stable shape. Thus,  $G'$  represents the elastic behavior of material and we shall name it elastic modulus.

**Viscous modulus (loss modulus)  $G''$  [Pa]** is a measure of deformation energy used during the shear process and lost to the sample. This energy is consumed for changes in the structure of material at the partial or complete flow of the sample. Flow or viscoelastic flow implies the relative movement between molecules, groups, particles, aggregates, and other structural components like domains or crystals. There are also friction forces between these components, which result in a temperature rise; this process is called viscous heating. During the friction, the energy is partially consumed for sample heating and partially dissipated into the environment. The materials showing irreversible deformation after the cycle of loads have a modified shape. Thus,  $G''$  represents a viscous behavior of the test sample; we shall name it viscous modulus.

**Linear viscoelastic (LVE) range.** At small amplitudes, the curves of  $G'$  and  $G''$  have ranges of constant values in the form of plateaus (Fig. 3), although usually on different levels. The load level to which the curves are parallel is called linear viscoelastic range.

**Damping factor** is calculated as the ratio of the viscous modulus to the elastic modulus and is equal to  $\tan \delta$ .

The viscoelastic behavior of any material consists of viscous and elastic behavior. In Fig. 4, the vector  $G'$  is on the axis  $x$ , and the vector  $G''$  is on the axis  $y$ .  $G^*$  is the sum of the vectors or the result of two components  $G'$  and  $G''$ ; it characterizes the complete viscoelastic behavior consisting of the both elastic and viscous components. The damping factor can be represented as the ratio of the side opposite to the angle  $\delta$  to the side adjacent to the angle  $\delta$ , i.e., the tangent of the angle  $\delta$ :  $\tan \delta = G''/G'$ .

The phase shift is equal to  $\tan \delta$ . Conditions for different behaviors of material are given in Table 1 [25].

**Integrated zone  $Z$ .** For the cumulative estimation of the stability range of structural bonds, it is proposed to calculate the area of the integrated zone  $Z$  from the damping factor, as the area limited by the initial value of shift amplitude on one side and  $\tan \delta < 1$  on the other size [22].

**Structural characterization of the sample.** In the description of sample properties, the following relationships can be used for the analysis of the sample behavior:

- a) if  $G' > G''$ , this is a solid substance, where elasticity prevails over viscosity; the sample shows some rigidity, as is typical for structured systems and stable pastes;
- b) if  $G' = G''$ , the values of the both moduli are balanced; this state (frequently named liquid limit) shows that the material is in the boundary state between liquid and solid;
- c) if  $G'' > G'$ , the viscous behavior prevails over the elastic behavior; the sample shows the character of the liquid. At rest, these materials are usually unstable and flow with time.

The structural or rheological characterization of samples was based on the following main parameters (Fig. 3):

1. At the beginning of the experiment, the value of elastic modulus at the lowest amplitudes characterizes the initial binding strength between particles in the studied sample.

2. At the low amplitudes (Fig. 3, phase I) in the region of linear viscoelasticity, each of the  $G'$  and  $G''$  curves has a range of constant values in the form of a plateau parallel to the axis  $x$ . The presence and range of this region indicate the stability of structural bonds in the sample under the set loads.

3. The next transitional region (Fig. 3, phase II) between the initial lowering points of the curves and their intersection is the region of plastic deformations. In this region, the substance behaves as a plastic body.

4. The intersection point of the curves (Fig. 3, phase III), or the equality  $G' = G''$ , indicates the transition of the sample from the viscoelastic to the viscous state (the fracture region of the elastic component of the sample, or deformation limit).

5. The integrated zone  $Z$  (Fig. 3, phases I and II) characterizes the total value of elastic and plastic behavior before the intersection point of the moduli.

## OBJECTS AND METHODS

The objects of study included the upper (0- to 10-cm) layers of typical chernozem (according to WRB, Haplic Chernozems (Pachic)) under unsown steppe, oak forest, long-term fallow, plowed field in agricultural use, and its adjacent forest belt.

The plots of unmown steppe, oak forest, and long-term fallow are located 100 km to the south of the city of Kursk in the Streletskaya Steppe of the Alekhin Central Chernozemic State Biospheric Reserve. The plot of long-term fallow 0.6 ha in area is located among the virgin herb-meadow steppe and has been tilled twice a year since 1947. Before tillage, this area of Streletskaya Steppe was used as a hayfield. The plot of plowland is located 9 km to the southeast of Kursk. The adjacent forest belt was planted on an old plowed field in 1976.

The chemical and physical properties of the Kursk chernozems are well understood and described in detail [3, 4, 17, 18]. The objects are located in the central part of the forest belt in the Seim River basin to the south of Kursk on the Central Russian Upland. The

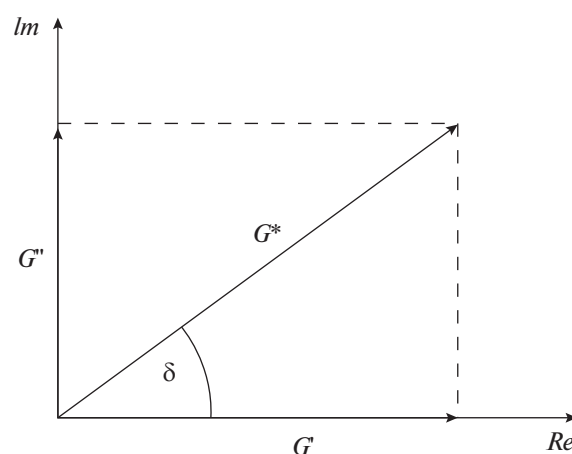


Fig. 4. Vector diagram for  $G'$ ,  $G''$ ,  $G^*$ , and  $\tan \delta$  ([25]).

area has a typical erosive topography. Loess-like loams are parent rocks. The reserve is located in the zone of temperate-cold climate and moderate moistening.

The particle size distribution in the studied soils was measured by the laser diffraction method on an Analysette 22 Comfort instrument after the dispersion of water-soil emulsion by ultrasound for 5 min [10]. From their particle size distribution, the soils are characterized as coarse-silty heavy loamy soils on loess-like loam according to the Kachinskii classification and as silt loam according to the USDA classification.

The content of total carbon was determined by dry digestion on an AN-7529 M analyzer [10]. The results are given in Table 2. The highest content of carbon was found in samples from unmown steppe, oak forest, and forest belt. The content of carbon in the soils of long-term fallow and plowland was almost two times lower.

The mineralogy of typical chernozems consists of labile minerals (46%) and chlorites (31%) [12].

The specific surface area was determined from water vapor desorption over salt solutions by the BET method [16]. The arable soils have the smallest specific surface area, which can be related to the content and properties of soil organic matter.

The soil water retention curve was determined by equilibrium centrifugation [11].

The rheological parameters of soil behavior were studied at the water contents corresponding to the maximum capillary water saturation and the liquid limit. Soil samples were preliminarily triturated with a

Table 1. Conditions for different behavior of materials ([25])

Ideal viscous flow	Viscoelastic liquid behavior	Viscoelastic behavior	Viscoelastic solid body behavior	Ideal elastic behavior
$\delta = 90^\circ$	$90^\circ > \delta > 45^\circ$	$\delta = 45^\circ$	$45^\circ > \delta > 0^\circ$	$\delta = 0^\circ$
$\tan \delta \rightarrow \infty$	$\tan \delta > 1$	$\tan \delta = 1$	$\tan \delta < 1$	$\tan \delta \rightarrow 0$
$G' \rightarrow 0$	$G'' > G'$	$G'' = G'$	$G' > G''$	$G'' \rightarrow 0$

**Table 2.** Some physical and chemical properties of soils

Sample	C <sub>tot</sub>	Clay (<0.001 mm)	Physical clay (<0.01 mm)	Swelling	Water content at maximum swelling	Water content at liquid limit	Specific surface area, m <sup>2</sup> /g
	%						
Unmown steppe	6.8	5.44	42.5	33.5	84.2	55.1	112.9
Oak forest	6.5	8.98	57.5	30.4	72.9	49.8	114.0
Forest belt	5.8	5.77	58.4	23.2	75.4	52.1	123.0
Plowland	3.3	8.14	49.4	16.5	63.6	39.9	98.8
Long-term fallow	3.0	9.7	53.2	17.2	56.5	35.7	86.6

rubber pest and sieved through a 0.25-mm sieve. Air-dry soil samples (3 g) were placed in small cylinders 2.5 cm in diameter, which corresponded to the diameter of the upper rheometer plate. The sample was leveled, slightly compacted, and put on a filter paper, the ends of which were sunk in distilled water for capillary saturation for 24 h. For the tests at the liquid limit, the air-dry soil was triturated, sieved through a 0.25-mm sieve, brought to the liquid limit by adding water, and controlled by the Vasil'ev fall-cone test [5]. The obtained paste was put in a plastic Petri dish 3 cm in diameter and left in a desiccator with saturated water vapor for 24 h for structuring.

The following technical test conditions were used: the distance between the plates  $h = \sim 2\text{--}4$  mm; the plate diameter = 2.5 cm; the shear deformation  $\gamma = 0.001\text{--}100\%$ ; the angular frequency  $f = 0.5$  Hz; the number of measuring points = 30; the sample temperature was maintained at a constant level of  $20^\circ\text{C}$  with Peltier units.

The tests were performed at two different conditions: (1) the sample thickness set at 3 mm and (2) the control of normal force  $<10$  N. In the former case, the instrument put pressure on the samples with an uncontrolled force; in the latter case, the control of normal force  $<10$  N was set. The experiments were performed in triplicate.

## RESULTS AND DISCUSSION

In the course of capillary water saturation, the soil samples adsorbed water and swelled. The highest swelling was observed for the samples with the maximum content of organic matter. The contents of total phosphorus and physical clay, the specific surface area, the water contents of maximum swelling (MS) and liquid limit (LL), and the values of sample swelling are shown in Table 2.

The MS water content on the soil water retention curves corresponds to the near-zero soil water pressure; the LL water content corresponds to the pressure of 1.1 pF (about  $-1300$  Pa). At zero pressure, water filled all pores of the soil samples; at the potential of 1.1 pF, the water content of the samples approximately corre-

sponds to the boundary between the free water state and the beginning of the action of capillary forces [6].

The first condition for the tests was the constant thickness of the sample equal to the distance between the plates (3 mm). To obtain the set distance, the rheometer applies a normal stress force to the sample between two plates and contracts it. The maximum force (22 N) was applied to the sample from the unown steppe to contract it to a thickness of 3 mm; then, the force decreased to 12 N for the oak forest, 10 N for the forest belt, and 4 N for the long-term fallow. These values of normal stress are in close correlation with the values of swelling, the coefficient of correlation being 0.92. The densities of samples with equal thicknesses varied: the higher the swelling or organic matter content, the higher the rheometer stress necessary to compact the sample to the set thickness and, hence, the higher the final density of the sample, the number of interparticle contacts, and the elastic modulus. Thus, the rheological parameters determined at the set thickness of the test sample a priori depend on the soil density rather than the natural interparticle interactions arising during capillary moistening. Therefore, the limit of normal stress force  $<10$  N was set; the sample thickness varied from 2 to 4 mm in this case. The values of elastic moduli for two test conditions in the region of linear viscoelasticity are shown in Fig. 5.

It can be seen (Fig. 5) that the elastic modulus at a constant sample thickness of 3 mm is significantly higher than that at the controlled normal force in all of the samples. It is possible that at the control of the sample thickness, soil particles in all samples are subjected to different compaction forces depending on sample swelling, and the measured parameters are first regulated by the artificially formed interparticle cohesion. At the control of normal force, the sample thickness varies, but the measured rheological parameters are regulated by the natural interparticle cohesion. Therefore, the rheological behavior of samples determined at the control of normal force  $<10$  N was analyzed later on at the study of natural interparticle cohesion.

Experiments were performed in triplicate; the average values are presented for discussion. The rheologi-



cal parameters—the linear viscoelastic range, the intersection point of moduli  $G' = G''$ , and the integrated zone  $Z$ —were calculated using the rheometer software. Recall that the linear viscoelastic range is the region of elastic behavior, where the  $G'$  and  $G''$  curves are parallel. The higher and larger this range, the better the interparticle interactions. The intersection point of the moduli  $G' = G''$  indicates the value of deformation corresponding to the transition of deformational behavior from viscoelastic to viscous. The value of the integrated zone  $Z$  indicates the total range of elastic and viscoelastic behavior; the higher this value, the stronger the interparticle bonds and the more stable the structure.

It can be seen (Fig. 6) that the strength of interparticle bonds in the linear viscoelastic range at the LL water content is 2–3 times higher than at the MS water content for all soil samples. The soil paste at the MS water content obviously contains more free water; therefore, particles occur at the maximum distance from one another, and the interparticle cohesion is low. The decrease in the content of water by 1.5 times (Table 2) apparently resulted in the development of capillary forces, which strengthened the interparticle cohesion by 2–3 times. The comparison of soils from different areas under anthropogenic use showed that the distribution of elastic moduli among the treatments at the initial test moment is similar at both water contents: the cohesion between soil particles is maximum in the long-term fallow and plowland and progressively decreases in the forest belt, the oak forest, and the unmown steppe. The interparticle interaction in the soils enriched with organic matter is lower than in the samples with the lower content of organic matter. The samples rich in organic matter probably adsorb and retain more water, which hampers the formation of close interparticle bonds and simultaneously acts as a lubricant and allows particles to be in freer motion relative to one another.

The linear viscoelastic ranges (Fig. 7) or the regions of elastic behavior at two levels of water content differ insignificantly, except for the fallow. The differentiation among the treatments is more manifested at the MS water content; the widest range is typical for the unmown steppe, and the narrowest range is observed for the long-term fallow. The structuring role of organic matter is obvious; its high content in the unmown steppe makes the soil resistant to loads even at the maximum water saturation. At the LL water content, which is about 1.5 times lower than the MS water content, the differentiation among the treatments is poorly manifested, probably because of capillary forces.

In the intersection point of the elastic and viscous moduli (Fig. 8), the value of deformation  $\gamma$  (%) corresponding to the transition of soil to the viscous state in the samples at the MS water content is significantly higher than in the samples at the LL water content. At the higher water content, the behavior of soils under

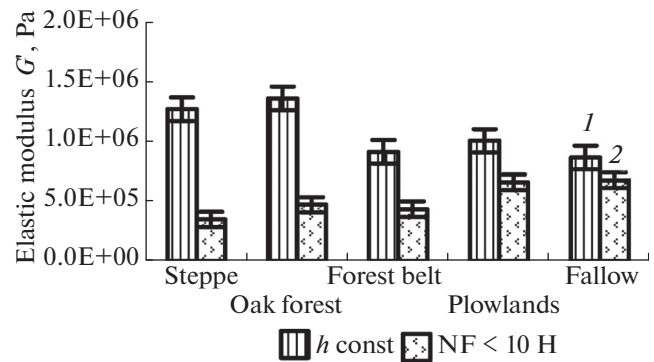


Fig. 5. Elastic moduli of samples in the undisturbed region (linear viscoelastic range) at (1) the constant sample thickness ( $h = 3$  mm) and (2) the controlled normal force ( $NF < 10$  N).

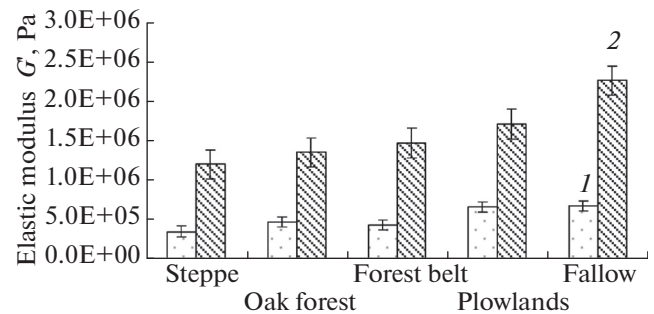
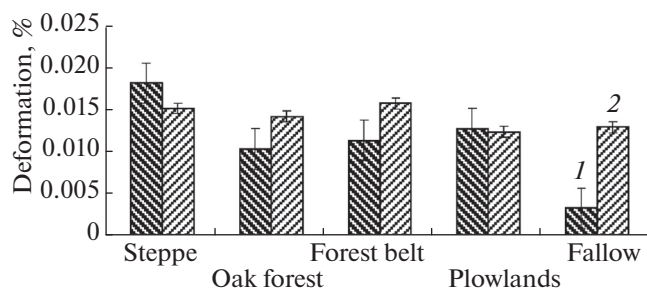


Fig. 6. Elastic moduli in the linear viscoelastic range at the water contents of (1) maximum swelling and (2) liquid limit.

load is more plastic than those at the LL water content. In the latter case, stronger interparticle bonds arise, but the rheological behavior of soil paste becomes more brittle, and the bonds are ruptured more rapidly than at the MS water content, because the soil particles are less capable of moving relative to one another. The highest plasticity and the widest range of viscoelastic structure are observed in the samples with the high content of organic matter.

The integrated zone  $Z$ , which represents the area limited by the initial shear amplitude from one side and the loss modulus curve from the other side to the intersection point equal to 1 (Fig. 9), can serve as an integrated parameter of viscoelastic behavior. The integrated zone  $Z$  corresponds to the total area of the regions of elastic and viscoelastic behavior before the transition to the viscous flow region. The higher the value of integral  $Z$ , the more viscoelastic the soil state.

It can be seen (Fig. 9) that the values of the integrated zone  $Z$  at two water contents are strongly different. At the MS water content or the soil water pressure close to 0, this zone is relatively large and distributed among the treatments as follows: unmown steppe > oak forest = forest belt > plowland > long-term fallow. At the LL water content or the soil water pressure of —



**Fig. 7.** Linear viscoelastic range: (1) maximum swelling; (2) liquid limit.

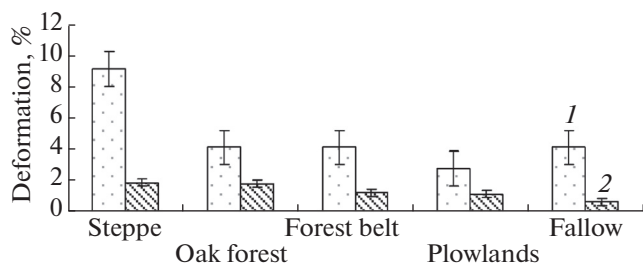


**Fig. 8.** Deformation in the intersection point of moduli  $G' = G''$  (the sample is in the boundary state between the plastic and viscous state) at the water contents of (1) maximum swelling and (2) liquid limit.

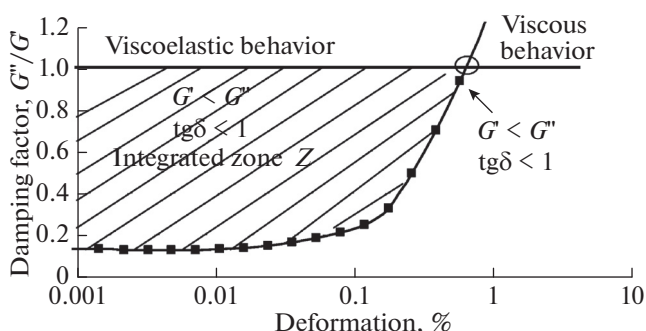


**Fig. 9.** Integrated zone Z of arable chernozem under long-term fallow.

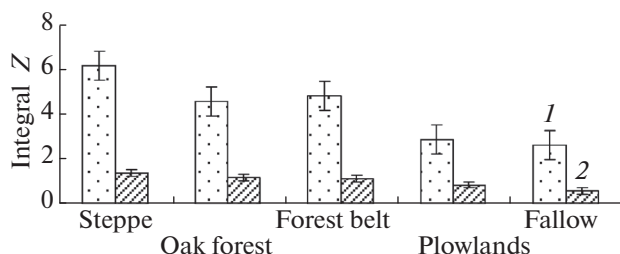


**Fig. 10.** Integrated zones Z at the water contents of (1) maximum swelling and (2) liquid limit.

1300 Pa, the zone of viscoelastic behavior is significantly smaller. The shift range of soil particles relative to one another abruptly decreased because of arisen capillary bonds. The distribution of the zone Z areas among the treatments completely corresponds to its distribution at the MS water content and is largely determined by the content of organic matter. Therefore, it may be concluded that organic matter favors the expansion of the range of viscoelastic soil behavior.

Thus, the rheological behavior of soils is largely determined by the content of organic matter, which can act as a binding agent structuring the interparticle bonds at the high water content and fulfil the antierosion function, as well as act as a lubricant hampering the formation of strong interparticle bonds in the mineral soil component, thus ensuring a favorable aggregate structure without cementation of mineral particles into blocks. The samples enriched with organic matter (virgin land, oak forest, forest belt) have a more plastic behavior and a higher resistance to loads. The samples with the lower content of organic matter (long-term fallow, plowland) have a more rigid interparticle cohesion and a narrower range of resistance to loads. Soil pastes at the LL water content are characterized by a higher strength of interparticle cohesion and a more brittle behavior than at the MS water content.

## CONCLUSIONS

1. The comparison of the rheological parameters of soil pastes from typical chernozems under different land use determined by the amplitude sweep method on an MCR-302 modular rheometer showed that the soil areas not subjected to anthropogenic impact (virgin land, oak forest, forest belt) are more resistant to loads, probably due to the structuring effect of organic matter (all other properties being relatively similar), which is confirmed by many authors [17, 18, 22, 24].

2. The rheological properties of soil under forest belt significantly differ from those of plowland and approach those of virgin plots, which indicates the restoration of the structural organization of soil particles under forest belt conditions.

3. The rheological behavior of soil pastes strongly depends on moistening conditions. At the high water content (MS), the rheological behavior of soils is largely determined by the content of organic matter, which acts as a binding agent structuring the interparticle bonds and thus increases the soil stability (water resistance in the saturated state), as well as fulfils antierosion functions by hampering the transition of soil to the flowing state

When the water content decreases, the strength of structural bonds increases abruptly and the range of the viscoelastic state is reduced. The soil pastes at the lower water content (LL) are characterized by a higher strength of interparticle cohesion and a more brittle behavior than at the MS water content. Organic matter acts as a lubricant, which hampers the formation of

strong (crystallization) interparticle bonds in the mineral soil component and thus ensures a favorable aggregate structure without cementation of mineral particles into blocks.

4. The methodological aspects of soil paste testing at the constant thickness of the soil sample and the controlled normal force applied to the sample are that the tests at the controlled normal force are preferable for swelling samples.

The organic matter of chernozems under studied conditions determines the formation and strength of interparticle bonds. The interparticle bonds in the water content range between LL and MS can be studied by the amplitude sweep method in oscillation mode on an MCR-302 modular rheometer with a parallel-plate measuring system (Anton-Paar, Austria). This method determines some quantitative parameters of the rheological behavior of soil samples, including the range of elastic behavior or the stable state of soil structure under increasing load and the region of transitional state or plastic behavior between the elastic and viscous regions. The method also provides the quantitative characteristic in pressure units (Pa) for the interparticle interaction at each stage of the rheological curve.

#### ACKNOWLEDGMENTS

This work was supported in part by the Russian Science Foundation (project no. 14-16-00065) and the Russian Foundation for Basic Research (project no. 11-04-01683).

#### REFERENCES

1. L. P. Abrukova, "Analysis of thixotropic properties of soils using rotational viscosimeter," *Pochvovedenie*, No. 8, 104–114 (1970).
2. V. V. Abrukova and A. S. Manucharov, "Rheological characteristics of surface gley soils," *Pochvovedenie*, No. 9, 44–52 (1986).
3. E. A. Afanas'eva, *Chernozems of the Central Russian Upland* (Nauka, Moscow, 1966) [in Russian].
4. G. S. Bazykina, "Analysis of the long-term dynamics of moisture balance components in typical chernozems of the reserved steppe area in Kursk region," *Eurasian Soil Sci.* **43** (12), 1362–1372 (2010).
5. A. F. Vadyunina and Z. A. Korchagina, *Manual for the Analysis of Soil Physical Properties* (Vysshaya Shkola, Moscow, 1973), p. 398.
6. A. D. Voronin, *Structural-Functional Hydrophysics of Soils* (Mosk. Gos. Univ., Moscow, 1984) [in Russian].
7. I. M. Gor'kova, *Physicochemical Study of Disperse Sedimentary Rocks for Construction Purposes* (Stroiizdat, Moscow, 1975) [in Russian].
8. T. A. Zubkova and L. O. Karpachevskii, *Matrix Organization of Soils* (Rusaki, Moscow, 2001) [in Russian].
9. A. S. Manucharov, "Use of rheological studies in soil science," *Vestn. Mosk. Univ.*, Ser. 17: *Pochvoved.*, No. 3, 56–40 (1983).
10. E. Yu. Milanovskiy, D. D. Khaidapova, A. I. Pozdnyakov, T. N. Pochatkova, and Z. Tyugai, *Practical Manual on Physics of Soil Solid Phase* (Grif i K, Moscow, 2011) [in Russian].
11. A. V. Smagin, "Column-centrifugation method for determining water retention curves of soils and disperse sediments," *Eurasian Soil Sci.* **45** (4), 416–422 (2012).
12. T. A. Sokolova, T. Ya. Dronova, and I. I. Tolpeshta, *Clay Minerals in Soils* (Grif i K, Tula, 2005) [in Russian].
13. D. D. Khaidapova, E. Yu. Milanovskiy, and V. V. Chestnova, "Rheological analysis of soil structure recovery under the impact of shelterbelts planted on the anthropogenically disturbed soils," *Vestn. Altai. Gos. Agrar. Univ.*, No. 6, 53–57 (2014).
14. D. D. Khaidapova and E. A. Pestonova, "Strength of interparticle bonds in soil pastes and aggregates," *Eurasian Soil Sci.* **40** (11), 1187–1192 (2007).
15. D. D. Khaidapova, Yu. V. Kholopov, I. V. Zaboeva, and E. M. Lapteva, "Rheological features of the coagulative structure of northern taiga peaty podzolic gleyed soils of the European Northeast," *Moscow Univ. Soil Sci. Bull.* **69** (1), 17–22 (2014).
16. E. V. Shein, T. A. Arkhangel'skaya, V. M. Goncharov, A. K. Guber, T. A. Pochatkova, M. A. Sidorova, A. V. Smagin, and A. B. Umarova, *Field and Laboratory Analysis of Physical Properties and Regimes of Soils* (Mosk. Gos. Univ., Moscow, 2001) [in Russian].
17. E. V. Shein, V. I. Lazarev, Y. Y. Aidiev, T. Sakunkonchak, Y. Y. Kuznetsov, Y. Y. Milanovskii, and D. D. Khaidapova, "Changes in the physical properties of typical chernozems of Kursk oblast under the conditions of a long-term stationary experiment," *Eurasian Soil Sci.* **44** (10), 1097–1103 (2011).
18. E. V. Shein, E. Yu. Milanovskiy, and D. D. Khaidapova, "Resistance of soil structure and soil organic matter," *Tr. Inst. Pochvoved.*, *Russ. Akad. Nauk*, No. 1, 129–151 (2002).
19. E. V. Shein, A. G. Bolotov, D. D. Khaidapova, E. Yu. Milanovskiy, Z. N. Tyugai, and T. N. Pochatkova, "Rheological properties of chernozems in Altai Ob region," *Vestn. Gos. Agrar. Univ.*, No. 8, 32–38 (2014).
20. G. Schramm, *A Practical Approach to Rheology and Rheometry* (Gebrueder Haake Verlag, Karlsruhe, 2000; Kolos, Moscow, 2003) [in Russian].
21. D. Khaidapova, E. Yu. Milanovskiy, and E. V. Shein, "Impact of anthropogenic load on rheological properties of typical chernozems (Kursk region, Russia)," in *Soil Degradation*, *Adv. Geocol. Ser. (Catena, Reiskirchen)*, 2013, No. 42, pp. 62–71.
22. W. Markgraf, R. Horn, and S. Peth, "An approach to rheometry in soil mechanics—structural changes in bentonite, clayey and silty soils," *Soil Tillage Res.* **91**, 1–14 (2006).
23. W. Markgraf, F. Moreno, and R. Horn, "Quantification of microstructural changes in salorthidic fluvaquents using rheological and particle charge techniques," *Vadose Zone J.* **11** (1), (2011). doi 10.2136/vzj2011.0061w
24. W. Markgraf, C. W. Watts, W. R. Whalley, T. Hrkac, and R. Horn, "Influence of organic matter on rheological properties of soil," *Appl. Clay Sci.* **64**, 25–33 (2012).
25. T. G. Mezger, *The Rheology Handbook* (Vincentz Network, Hanover, 2011)

Translated by K. Pankratova